Appendix 1 to Milella MS, Fotros A, Gravel P, et al. Cocaine cue–induced dopamine release in the human prefrontal cortex. *J Psychiatry Neurosci* 2016.

DOI: 10.1503/jpn.150207

Online appendices are unedited and posted as supplied by the authors.

Supplemental Material

1. Measuring cortical and striatal dopamine release together

Despite the interest in cortical function, measuring DA release in the human brain has been largely limited to the striatum. First generation D2/D3 PET radio-ligands, such as [^{11}C]raclopride [1], have been used extensively but they allow confident investigation of the striatum only, a region where D2/D3 receptors are in abundance. Second generation radio-ligands have overcome this limitation, extending PET quantification to brain regions with lower receptor concentrations. One of these tracers is [^{18}F]fallypride [(S)-N-[(1-allyl-2-pyrrolidinyl)methyl]-5-(3-[^{18}F]fluoropropyl)-2, 3-dimethoxybenzamide], a substituted benzamide compound with a favorable pharmacokinetic profile by virtue of the higher affinity for D2/D3 receptors (*in vitro* K_D 0.03 nmol/L and *in vivo* K_D 0.2 nmol/L) [2,3], higher selectivity for D2, longer half-life, and rapid clearance from nonspecific binding sites, ensuring a superior signal-to-noise ratio [3,4,5]. In particular, the long half-life of fluorine-18 (110 min) allows the measurement of D2/D3 availability in extrastriatal and striatal regions simultaneously in a single session. The levels of [^{18}F]fallypride binding in striatal and extrastriatal regions, including the PFC, are in agreement with *in vitro* autoradiography and *in vivo* distribution studies of D2/D3 receptors [6,7,8].

2. Radiosynthesis of [^{18}F]fallypride

[^{18}F]Fallypride was prepared by simple nucleophilic substitution of a fallypride tosyl (ABX, Germany) with ^{18}F- and with a final HPLC purification and reformulation of the pure radiotracer. The dose administered was in the range of 3.0 mCi to 3.8 mCi (3.33 ± 0.24 mCi for scan 1; and 3.28 ± 0.24 mCi for scan 2). Furthermore, for all the scans the specific activity was in the range 900-1200 Ci/mmol. Considering the mean injected dose for each scan, the mass dose administered was in the range of 1.01 μg to 1.35 μg for scan 1 and 1.00 μg to 1.33 μg for scan 2.

3. Positron emission tomography image reconstruction

Reconstructions were performed using OP-OSEM (Ordinary Poisson Ordered Subset Expectation Maximization: 10 iterations, 16 subsets) [9,10] including compensation for dead-time, detector non-uniformities, attenuation, scattered and random coincidences and motion. The reconstructed image frames were composed of 256×256×207 voxels (voxel side length = 1.21875 mm). Motion correction for repositioning errors and potential head movement during the scans was based on an image-based automated algorithm [11] that estimates rigid-body motion between the dynamic frames. Emission data were then re-reconstructed taking into account mismatch between the transmission scan and each individual emission frame. The emission images for the different frames were then realigned to a common head position.

4. ROI segmentation

Each participant underwent T_1-weighted MRI imaging for the purpose of PET/MR co-registration. The MRIs were obtained on a Siemens 1.5 tesla Sonata scanner from a 3D fast field echo sequence with sagittal

Appendix 1 to Milella MS, Fotros A, Gravel P, et al. Cocaine cue–induced dopamine release in the human prefrontal cortex. *J Psychiatry Neurosci* 2016.

DOI: 10.1503/jpn.150207

Online appendices are unedited and posted as supplied by the authors.

acquisition and 160 slices at 1mm isotropic resolution (TR = 9.7 ms, TE = 4 ms, flip angle = 12°, FOV = 250 and matrix 256 × 256). Each MR image was first pre-processed with CIVET pipeline (version 1.1.9) (www.bic.mni.mcgill.ca/ServicesSoftware/CIVET) developed at the MNI for fully automated structural image analysis [47]. The native MR volume was normalized for intensity, corrected for non-uniformity, and linearly and non-linearly transformed into standardized stereotaxic space using automated feature-matching [12] to the ICBM152 template. The MR image in stereotaxic space was classified into white matter, gray matter and CSF, and was automatically segmented in main brain structures using a probabilistic atlas based approach (ANIMAL) [13]. Through this approach, the prefrontal ROIs investigated here were identified: the medial orbito-frontal gyrus (mOFC), the lateral orbito-frontal gyrus (latOFC), the dorsolateral PFC (comprising of the superior, middle and inferior frontal gyrus, DLPFC), and the medial frontal gyrus (mPFC). The anterior cingulate cortex (ACC), SN and VTA were segmented as specified (Fig S1 and S2). Functional subdivision of the striatum (ventral, VST; associative, AST and sensorimotor, SMST) was performed as previously described [14,15]. Each ROI was resampled to the PET reconstruction space and eroded around its edges by 1 voxel.

The spatial rigid-body transformation between the summed PET volume and the native MR image was estimated with normalized mutual information, and was used to position the ROI masks into the native PET space. The resulting registration was visually checked for the whole brain and at the level of basal ganglia.

4.1 Anterior cingulate

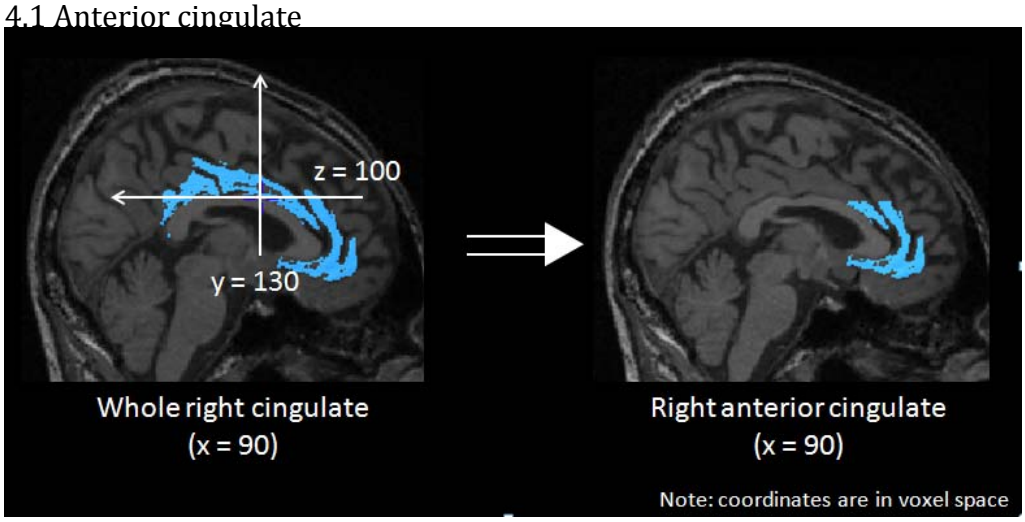

Figure S1. Anterior cingulate segmentation in stereotaxic (STX) space, using CIVET. Axial planes (*z*-direction) greater than or equal to 100 were set to 0, as well as coronal planes lower or equal to 130, leaving the ROI shown on the right hand side.

Appendix 1 to Milella MS, Fotros A, Gravel P, et al. Cocaine cue–induced dopamine release in the human prefrontal cortex. *J Psychiatry Neurosci* 2016.

DOI: 10.1503/jpn.150207

Online appendices are unedited and posted as supplied by the authors.

4.2 SN/VTA

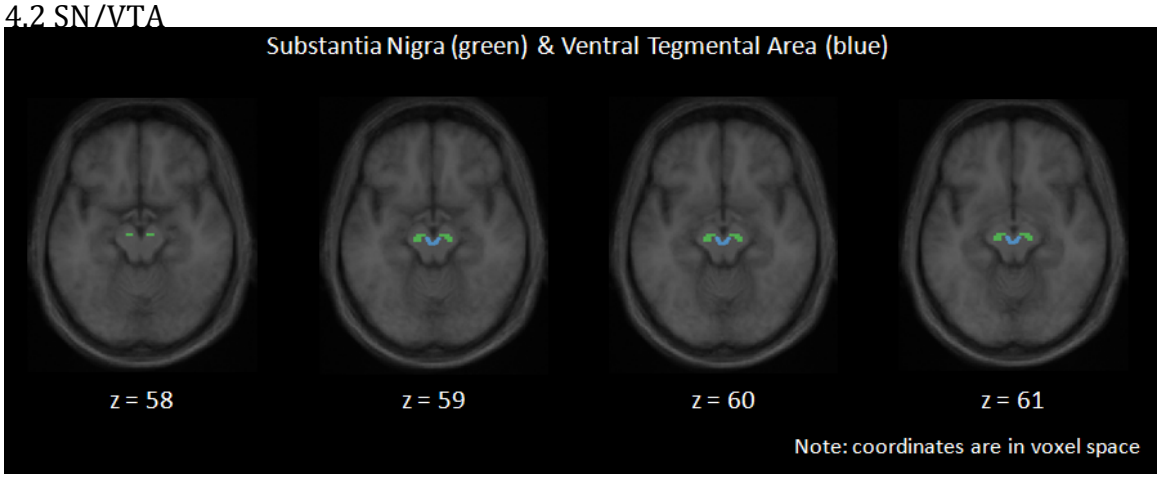

Figure S2. Substantia nigra (SN, green) and ventral tegmental area (VTA, blue) segmentation superimposed on the average MRI in STX space of the 12 participants. SN was defined as in Gravel [16]. Using the SN as a guideline, the VTA was drawn manually based on Blumenfeld (2010).

Appendix 1 to Milella MS, Fotros A, Gravel P, et al. Cocaine cue–induced dopamine release in the human prefrontal cortex. *J Psychiatry Neurosci* 2016.

DOI: 10.1503/jpn.150207

Online appendices are unedited and posted as supplied by the authors.

Table S1: Self-Reported Drug Use

Drug Class	Mean	St. Dev	Number of users
Alcohol (intoxication)			
Age of First Use	14.7	2.99	12
Lifetime days of use	1464.3	1595.1	12
Avg. uses per year	77.1	120.5	8
Uses past 30 days	7.5	10.5	8
Cannabis			
Age of First Use	16.8	3.99	12
Lifetime days of use	2579.1	3297.03	12
Avg. uses per year	122.25	153.8	8
Uses past 30 days	15.8	12.8	8
Amphetamines			
Age of First Use	28	13.2	4
Lifetime days of use	15.25	17.03	4
Avg. uses per year	150	0	1
Uses past 30 days	1	0	1
MDMA			
Age of First Use	23.5	6.02	6
Lifetime days of use	16.16	18. 7	6
Avg. uses per year	1	0	1
Uses past 30 days	1	0	1
Tobacco			
Age of First Use	17.4	6.5	11
Uses past 30 days	365	0	9
Cigarettes/Day	11.7	6.64	9

Appendix 1 to Milella MS, Fotros A, Gravel P, et al. Cocaine cue–induced dopamine release in the human prefrontal cortex. *J Psychiatry Neurosci* 2016.

DOI: 10.1503/jpn.150207

Online appendices are unedited and posted as supplied by the authors.

5. Time-activity curves (TAC)

The lengthy PET protocol included a break after 90 min of acquisition to minimize discomfort. Then subjects were carefully repositioned in the scanner. The motion correction software algorithm corrected for possible misalignments [11].

Shown below are the TACs for the OFC (left) and sensorimotor striatum (right) ROI for a representative subject, on the cocaine cues session. No marked alteration from the fitting of the PET signal is visible at 120 min when the session resumed after the break. Additional TAC plots are available upon request.

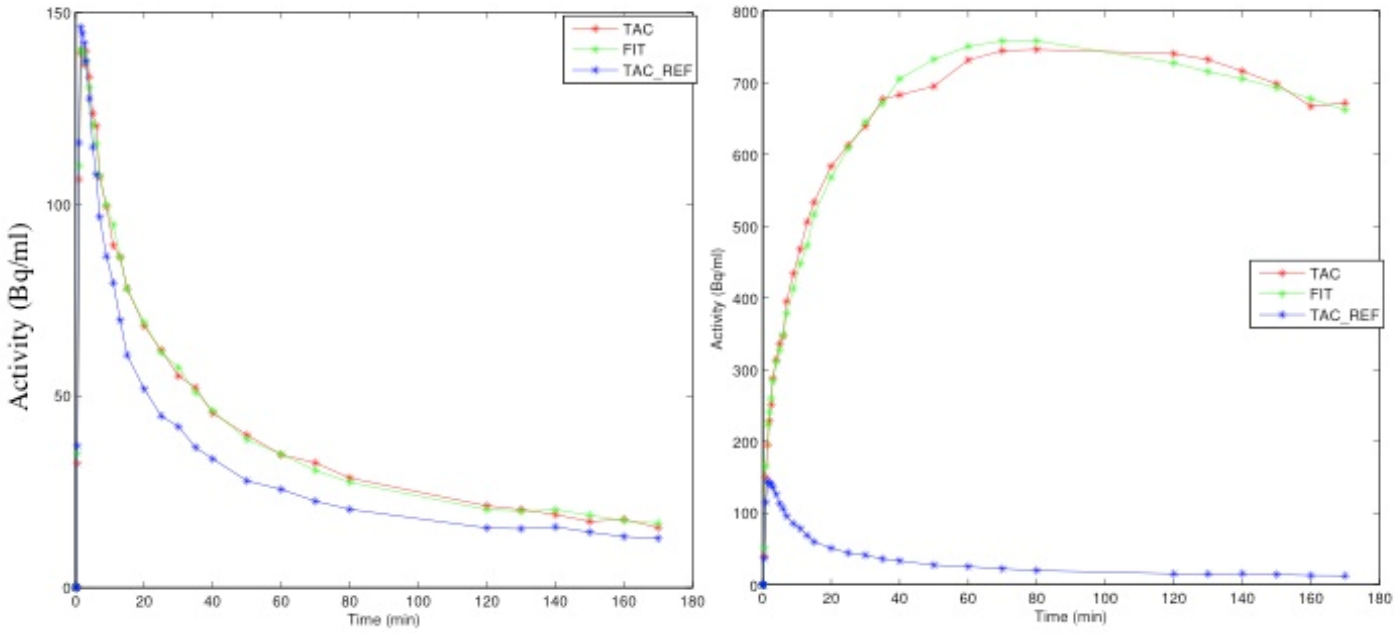

Figure S3. Time-activity curves (TAC) are presented in red. Fitting lines derived from the simplified reference tissue model are presented in green. Cerebellum TAC is presented in blue.

Appendix 1 to Milella MS, Fotros A, Gravel P, et al. Cocaine cue–induced dopamine release in the human prefrontal cortex. *J Psychiatry Neurosci* 2016.

DOI: 10.1503/jpn.150207

Online appendices are unedited and posted as supplied by the authors.

6. Supplemental analysis

We here present additional statistical analysis on the sample. To rule out the possibility that individual differences in the cue-induced changes in BP_{ND} values did not reflect different baseline values, ΔBP_{ND} was regressed against baseline BP_{ND} values in each of the ROIs, and no relationship was found in cravers (R^2s ≤ 0.25, except in the mPFC, R^2 = 0.39 and DLPFC, R^2 = 0.41, All p-values ≥ 0.07), or in the whole sample (for mOFC, R^2 = 0.031, ACC = 0.004, all others R^2s ≤ 0.202). A Bland-Altman plot for the two BP_{ND} measures (on neutral and cue session) is presented below.

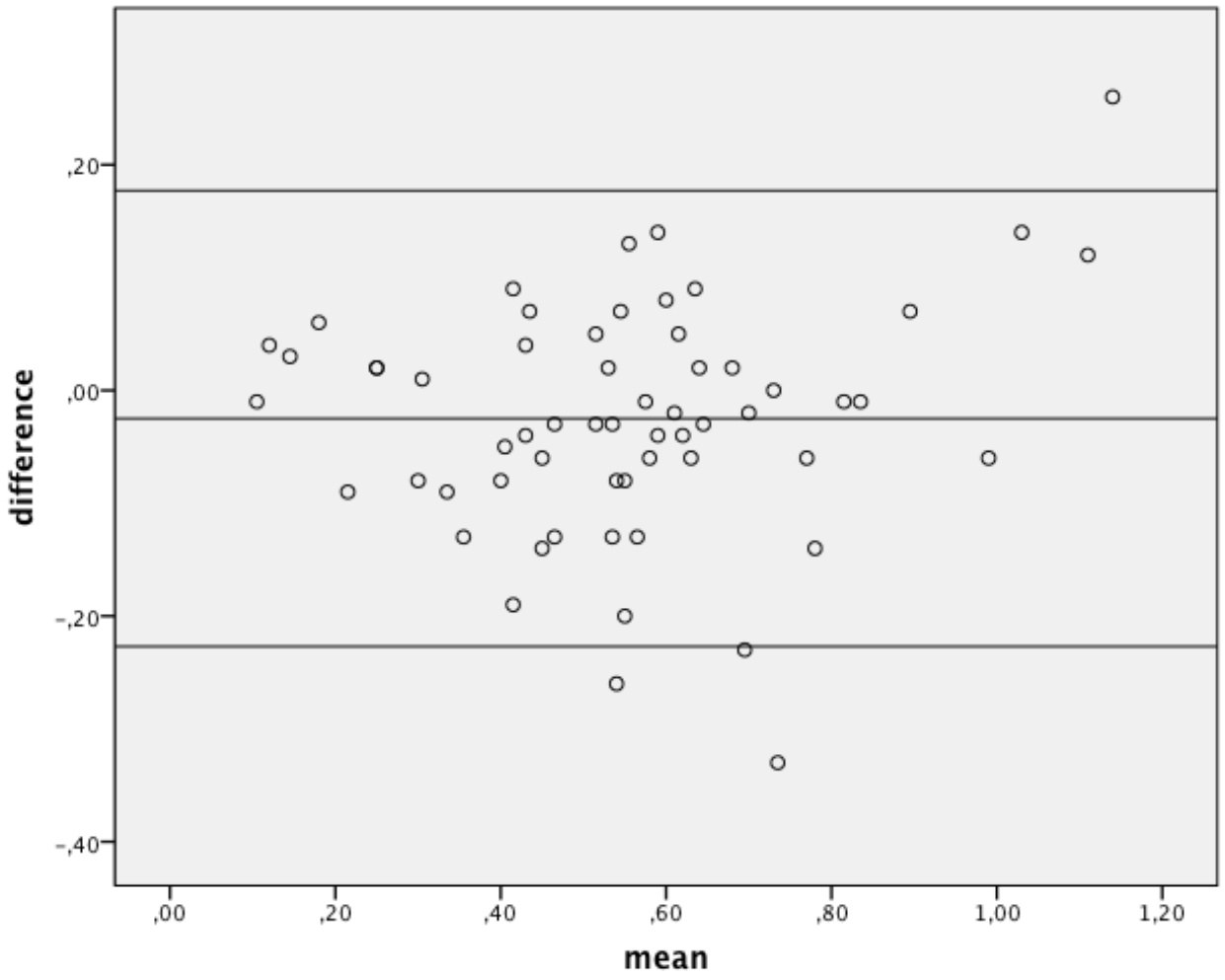

Figure S4. Bland-Altman plot. The Y-axis is the difference between BP_{ND} values on neutral and cue session. The X-axis is the mean of the two measures. The horizontal lines show the average difference (central line) and the 95% confidence interval (upper and lower lines).

Appendix 1 to Milella MS, Fotros A, Gravel P, et al. Cocaine cue–induced dopamine release in the human prefrontal cortex. *J Psychiatry Neurosci* 2016.

DOI: 10.1503/jpn.150207

Online appendices are unedited and posted as supplied by the authors.

A 3-way ANOVA, including 'Group' (cravers n = 9, and non-cravers n = 3) as a between subject factor, was performed. Within the cortex, there were statistically significant Group x Session ($F_{(1,22.13)} = 9.96$, p = 0.010; partial $\eta^2 = 0.499$) and Group × Session × ROI interactions ($F_{(2.21,22.13)} = 3.31$, p = 0.050; partial $\eta^2 = 0.294$). Examination of the three-way interaction indicated that it reflected the ability of cocaine cues to decrease BP_{ND} values in cocaine cravers, but not non-cravers, in the mOFC (p = 0.010; Cohen's *d*: 0.54; CI: 0.67 – 0.39) and ACC (p = 0.040; Cohen's *d*: 0.42; CI: 0.51 – 0.31).

Group × Session ($F_{(1,12.97)} = 5.35$, p = 0.043; partial $\eta^2 = 0.349$) and Group × Session × ROI interactions were also seen in the striatum ($F_{(1.29,12.97)} = 4.89$, p = 0.038; partial $\eta^2 = 0.328$), reflecting significant effects in the VST (p = 0.024) and SMST (p = 0.046), as described in additional detail elsewhere (Fotros et al. 2013).

Among the 12 subjects, only one had cortical ROI BP_{ND} values <0.20 (Subject #16, range 0.10 – 0.21, anterior cingulate excluded). The same range of BP_{ND} values was seen at both Day1 and Day 2 PET scans for this individual, suggesting this was not due to technical/acquisition or radio-tracer production issues. Nevertheless, the low signal-to-noise ratio in the cortex might have affected the reliability of these 'low-end' values. Excluding the subject from the sample does not change any of the effects shown (2-way repeated measures ANOVA Group × Session interaction: $F_{(1,9)} = 12.63$, p = 0.006; Group × Session × ROI interaction: $F_{(1,36)} = 2.96$, p = 0.033; post-hoc LSD: mOFC p = 0.010, ACC p = 0.031).

The two groups did not differ in age, age of first cocaine use, years of cocaine use, frequency and amount of use, hours since last use, or BDI or CSSA scores (p > 0.1).

There was a positive trend between hours since last use and the craving response (r = 0.54, p = 0.066), although no correlation with BP_{ND} changes was found (all $r \leqslant 0.41$, $p \geqslant 0.18$). Cocaine withdrawal severity (CSSA scores) at the start of the cocaine session was not associated with craving (r = 0.28, p = 0.37) nor with BP_{ND} changes in any of the regions tested (all $r \leqslant 0.35$, $p \geqslant 0.25$).

References:

1 Farde L, Hall H, Ehrin E et al. Quantitative analysis of D2 dopamine receptor binding in the living human brain by PET. *Science* 1986; 231:258-261.
2 Mukherjee J, Yang ZY, Das MK et al. Fluorinated benzamide neuroleptics--III. Development of (S)-N-[(1-allyl-2-pyrrolidinyl)methyl]-5-(3-[18F]fluoropropyl)-2, 3-dimethoxybenzamide as an improved dopamine D-2 receptor tracer. *Nucl Med Biol* 1995; 22:283-296.
3 Slifstein M, Hwang DR, Huang Y et al. In vivo affinity of [18F]fallypride for striatal and extrastriatal dopamine D2 receptors in nonhuman primates. *Psychopharmacology* 2004; 175:274-286.

Appendix 1 to Milella MS, Fotros A, Gravel P, et al. Cocaine cue–induced dopamine release in the human prefrontal cortex. *J Psychiatry Neurosci* 2016.

DOI: 10.1503/jpn.150207

Online appendices are unedited and posted as supplied by the authors.

4 Mukherjee J, Yang ZY, Brown T et al. Preliminary assessment of extrastriatal dopamine D-2 receptor binding in the rodent and nonhuman primate brains using the high affinity radioligand, 18F-fallypride. *Nucl Med Biol* 1999; 26:519-527.

5 Christian BT, Narayanan T, Shi B et al. Measuring the in vivo binding parameters of [18F]-fallypride in monkeys using a PET multiple-injection protocol. *J Cereb Blood Flow Metab* 2004; 24:309-322.

6 Hall H, Sedvall G, Magnusson O et al. Distribution of D1- and D2-dopamine receptors, and dopamine and its metabolites in the human brain. *Neuropsychopharmacology* 1994; 11:245-256.

7 Hall H, Farde L, Halldin C et al. Autoradiographic localization of extrastriatal D2-dopamine receptors in the human brain using [125I]epidepride. *Synapse* 1996; 23:115-123.

8 Abi-Dargham A, Hwang DR, Huang Y et al. Quantitative analysis of striatal and extrastriatal D2 receptors in humans with 18F-fallypride: validation and reproducibility. *Neuroimage* 2000. 11:S43

9 Comtat C, Bataille F, Michel C et al. OSEM-3D reconstruction strategies for the ECAT HRRT. In: *Nuclear Science Symposium Conference Record*, 2004 IEEE, vol. 6, pp 3492-3496 Vol. 3496.

10 Hong IK, Chung ST, Kim HK et al. Ultra fast symmetry and SIMD-based projection-backprojection (SSP) algorithm for 3-D PET image reconstruction. *IEEE transactions on medical imaging* 2007; 26:789-803.

11 Costes N, Dagher A, Larcher K et al. Motion correction of multi-frame PET data in neuroreceptor mapping: simulation based validation. *NeuroImage* 2009; 47:1496-1505.

12 Collins DL, Neelin P, Peters TM et al. Automatic 3D intersubject registration of MR volumetric data in standardized Talairach space. *J Comput Assist Tomogr* 1994; 18:192-205.

13 Collins DL, Evans AC. Animal: Validation and Applications of Nonlinear Registration-Based Segmentation. *Int J Patt Recogn Artif Intell* 1997; 11:1271-1294.

14 Fotros A, Casey KF, Larcher K et al. Cocaine cue-induced dopamine release in amygdala and hippocampus: a high-resolution PET [18F]fallypride study in cocaine dependent participants. *Neuropsychopharmacology* 2013; 38:1780-1788.

15 Martinez D, Slifstein M, Broft A et al. Imaging human mesolimbic dopamine transmission with positron emission tomography. Part II: amphetamine-induced dopamine release in the functional subdivision of the striatum. *J Cereb Blood Flow* 2003; 23:285-300.

16 Gravel P. Positron Emission Tomography of Extra-Striatal Dopamine Release. M.Sc. Thesis, McGill University. Montreal (QC) 2008; pp.1-100.